

Experimentally determined correlation between direct and inverse Edelstein effects at Bi₂O₃/Cu interface by means of spin absorption method using lateral spin valve structure

Hironari Isshiki¹, Prasanta Mudli¹, Junyeon Kim², Kouta Kondou², YoshiChika Otani^{1,2},

¹ Institute for Solid State Physics, University of Tokyo, Kashiwa, Chiba 277-8581, Japan

² Center for Emergent Matter Science, RIKEN, Wako, Saitama 351-0198, Japan

Abstract

We have experimentally elucidated the correlation between inverse and direct Edelstein Effects (EEs) at Bi₂O₃/Cu interface by means of spin absorption method using lateral spin valve structure. The conversion coefficient λ for the inverse EE is determined by the electron momentum scattering time in the interface, whereas the coefficient q for the direct EE is by the spin ejection time from the interface. For the Bi₂O₃/Cu interface, the spin ejection time was estimated to be ~ 53 fs and the momentum scattering time ~ 13 fs at room temperature, both of which contribute to the total momentum relaxation time that defines the resistivity of the interface. The effective spin Hall angle for the Bi₂O₃/Cu interface amounts to $\sim 10\%$ which is comparable to commonly used spin Hall material such as platinum. Interesting to note is that the experimentally obtained Edelstein resistances given by the output voltage divided by the injection current for direct and inverse effects are the same. Analysis based on our phenomenological model reveals that the larger the momentum scattering time, the more efficient direct EE; and the smaller spin ejection time, the more efficient inverse EE.

The spin-charge current interconversion via inverse and direct EE at interface [1] has recently attracted much attention due to its qualitatively different conversion mechanism than the bulk spin Hall effect [2]. These conversions are attributed to the spin-momentum locking at the interface where the electron spins are orthogonally coupled to their momenta by Rashba effect (See Fig. 1(a)) [3] or the topological nature of topological insulators. In the inverse Edelstein effect (IEE), the in-plane polarized 3D spin current $j_{s_IEE}^{3D}$ [A/m²] injected into the interface can be converted to the 2D charge current $j_{c_IEE}^{2D}$ [A/m] flowing orthogonal to the spin polarization direction of the spin current. For IEE caused by Rashba type spin-orbit coupling, the spin-to-charge conversion coefficient i.e. Edelstein length in the length unit meters λ can be expressed as [4,5],

$$\lambda \equiv \frac{j_{c_IEE}^{2D}}{j_{s_IEE}^{3D}} \sim \frac{\alpha_R \tau_{IEE}}{\hbar} \text{ [m]}. \quad (1)$$

Here, \hbar is the Dirac constant and α_R is the Rashba parameter of the interface and τ_{IEE} is the momentum scattering time inside the 2D interfacial conductive layer.

In the direct Edelstein effect (DEE), 2D charge current $j_{c_DEE}^{2D}$ [A/m] flowing in the interface produces a spin accumulation, a part of which diffuse into the adjacent bulk region, resulting in a 3D spin current $j_{s_DEE}^{3D}$ [A/m²] whose spin polarization direction is perpendicular to the flow of $j_{c_DEE}^{2D}$. The charge-to-spin conversion coefficient for the DEE is given by $q \equiv j_{s_DEE}^{3D}/j_{c_DEE}^{2D}$ [m⁻¹] [6]. The DEE is an important mechanism to produce the spin current exerting the spin orbit torque on adjacent ferromagnetic layer [7]. It is therefore important to clarify the responsible physical parameters that maximize the coefficient q . For this purpose, we developed a phenomenological model for spin-charge interconversion through IEE and DEE by considering two kinds of relaxation times. Furthermore, we have applied the model for explaining the IEE and DEE at the Bi₂O₃/Cu interface [8–12], that were measured experimentally by spin absorption method. Our model provides a comprehensive understanding of spin-charge interconversion mechanism through IEE and DEE. The phenomenological expression of q is deduced by considering simple parabolic dispersion of spin-split band as shown in Fig. 1(a). The spin accumulation $\langle \delta S \rangle$ produced by $j_{c_DEE}^{2D}$ at an interface with α_R can be approximated as [13]

$$\langle \delta S \rangle \sim \frac{m \alpha_R}{g e \hbar E_F} j_{c_DEE}^{2D}. \quad (2)$$

Here, g is Landé g -factor, e is elementary charge, m and E_F are respectively effective mass of the electron and the Fermi energy of the interface state. Note that Eqs. (1) and (2) are valid in the high-density regime where the Fermi energy E_F is much larger than the spin orbit coupling $\alpha_R^2/2\hbar^2m$. On the other hand, when $E_F \leq \alpha_R^2/2\hbar^2m$ in the low density regime, neither Eq. (1) nor (2) is valid because the perturbative treatment of the spin orbit coupling fails [14,15]. We therefore only consider the high-density regime.

Considering that the accumulated spins $\langle \delta S \rangle$ at the interface are ejected to (or diffuse into) 3D

bulk with the probability of $1/\tau_{\text{DEE}}$ where τ_{DEE} is the spin ejection time across the interface, the spin current $j_{s_{\text{DEE}}}^{3\text{D}}$ can be given by

$$j_{s_{\text{DEE}}}^{3\text{D}}/e = \langle \delta S \rangle / \tau_{\text{DEE}}. \quad (3)$$

From Eqs. (2) and (3) with $E_{\text{F}} \sim mv_{\text{F}}^2/2$, $v_{\text{F}} = \hbar k_{\text{F}}/m$, and corresponding Fermi wavevector k_{F} in the interface state [16]), we obtain the conversion coefficient as,

$$q \equiv \frac{j_{s_{\text{DEE}}}^{3\text{D}}}{j_{c_{\text{DEE}}}^{2\text{D}}} \sim \frac{\alpha_{\text{R}}}{v_{\text{F}}^2 \hbar \tau_{\text{DEE}}} [\text{m}^{-1}]. \quad (4)$$

In this way, it is understood that the coefficients λ and q are respectively characterized by two kinds of relaxation times τ_{IEE} and τ_{DEE} (see Fig. 1(b)). It should also be noted that both τ_{IEE} and τ_{DEE} give the *total* momentum scattering time τ_{total} as

$$\frac{1}{\tau_{\text{total}}} = \frac{1}{\tau_{\text{IEE}}} + \frac{1}{\tau_{\text{DEE}}}. \quad (5)$$

In the Edelstein effects with the surface states of topological insulators, the conversion coefficients are expressed as

$$\lambda = v_{\text{F}} \tau_{\text{IEE}} [\text{m}], \quad (6)$$

$$q = 1/v_{\text{F}} \tau_{\text{ej}} [\text{m}^{-1}], \quad (7)$$

which correspond to Eqs. (1) and (4), respectively [17].

We measured DEE and IEE at $\text{Bi}_2\text{O}_3/\text{Cu}$ interface by means of non-local spin absorption method [18]. In this technique, we use a modified lateral spin valve structure as shown in the illustration of Figs. 2 (a) and (b) in which a 200-nm-wide $\text{Bi}_2\text{O}_3(10 \text{ nm})/\text{Cu}$ ($t_{\text{Cu}} = 12.9 \text{ nm} - 23.1 \text{ nm}$) middle wire is inserted in between the two ferromagnetic $\text{Ni}_{80}\text{Fe}_{20}$ (NiFe) wires that are 100-nm-wide and 30-nm-thick. These three wires are bridged by a 100-nm-wide and 100-nm-thick Cu wire. The details of device design and fabrication procedure are described in the supplemental material. The measurements were carried out at 10 K by means of lock-in detection with 173 Hz. In the IEE measurement, charge current $I_{\text{C}_{\text{IEE}}}$ of 500 μA flowing between NiFe and Cu wires builds up spin accumulation which drives a diffusive spin current along the Cu wire. A part of spin current is absorbed into the middle wire where the spin current is converted to the charge current via IEE, resulting in non-local voltage V_{IEE} along the middle wire. In the DEE measurement, the charge current $I_{\text{C}_{\text{DEE}}}$ of 500 μA flowing along the middle wire generates spin accumulation via DEE at the $\text{Bi}_2\text{O}_3/\text{Cu}$ interface which drives spin current propagating diffusively through the bridging Cu wire. The non-local voltage V_{DEE} between the NiFe wire and the Cu wire can then be detected. The IEE (DEE) resistance is defined as $R_{\text{IEE}} = V_{\text{IEE}}/I_{\text{C}_{\text{IEE}}}$ ($R_{\text{DEE}} = V_{\text{DEE}}/I_{\text{D}_{\text{IEE}}}$). The R_{IEE} and R_{DEE} vs magnetic field H for the middle wire with different Cu thickness t_{Cu} are shown in Fig. 2 (c). We found that the magnitude of inverse and direct Edelstein resistances ΔR_{IEE} and ΔR_{DEE} are always the same for all

the device with different t_{Cu} , whose trend is similar to that of the spin absorption measurements in spin Hall materials [19]. In our experiment, ΔR_{IEE} and ΔR_{DEE} reach the largest value of 0.080 m Ω when the copper thickness t_{Cu} is 18.9 nm.

Before considering DEE and IEE, we discuss the *effective* conversion efficiency of $\text{Bi}_2\text{O}_3/\text{Cu}$ middle wire which is assumed to be a single spin Hall material with *effective* inverse and direct spin Hall angles θ_{ISHE}^* and θ_{DSHE}^* , respectively. We used the equations described in Ref. [20] to calculate θ_{ISHE}^* , which were based on 1D spin diffusion model. The shunting factor x for our $\text{Bi}_2\text{O}_3/\text{Cu}$ wires were numerically calculated to be 0.097, 0.136, 0.166, 0.203, 0.242 and 0.281 for the samples with Cu thickness in the middle wires of 12.9 nm, 15.9 nm, 17.1 nm, 18.9 nm, 21.9 nm and 23.1 nm, respectively, by using SpinFlow3D [21]. We also separately calculated θ_{DSHE}^* from the direct measurements. The details of the calculation of θ_{DSHE}^* is described in supplemental material. Both of θ_{DSHE}^* and θ_{ISHE}^* take negative values, the magnitude of which are shown as a function of t_{Cu} in Fig. 3(a). We found $\theta_{\text{DSHE}}^* = \theta_{\text{ISHE}}^*$ for all of our samples, satisfying the Onsagar's reciprocity as in Ref. [19] that is natural consequence from the experimental results, $\Delta R_{\text{DEE}} = \Delta R_{\text{IEE}}$. The fact that θ_{DSHE}^* and θ_{ISHE}^* were calculated independently from the direct and inverse measurements together with the above-mentioned result, $\theta_{\text{DSHE}}^* = \theta_{\text{ISHE}}^*$ ascertain our calculation of θ_{DSHE}^* . The maximum value of the *effective* spin Hall angle is ~ 0.10 that is relatively large, assuring that $\text{Bi}_2\text{O}_3/\text{Cu}$ interface has great potential as spin current generator and detector.

λ can be calculated from the definition of Eq. (1) as [22],

$$\lambda = \frac{t_{\text{Cu}} w_{\text{M}}}{\rho_{\text{M}} x} \left(\frac{I_{\text{C,IEE}}}{I_{\text{S,IEE}}} \right) \Delta R_{\text{IEE}}, \quad (8)$$

where ρ_{M} is the resistivity of the middle wire, w_{M} is the width of the middle wire and $\overline{I_{\text{S,IEE}}}$ is the spin current injected into the interface. The injected spin current into the middle wire $I_{\text{S,IEE}}$ is given by

$$I_{\text{S,IEE}} = \frac{2PI_{\text{C,IEE}} \left(\frac{R_{\text{NiFe}}}{R_{\text{Cu}}} \right) \left[\sinh\left(\frac{L}{l_{\text{Cu}}}\right) + \left(\frac{R_{\text{NiFe}}}{R_{\text{Cu}}} \right) \exp\left(\frac{L}{l_{\text{Cu}}}\right) \right]}{\left\{ \cosh\left(\frac{L}{l_{\text{Cu}}}\right) - 1 \right\} + 2\left(\frac{R_{\text{M}}}{R_{\text{Cu}}}\right) \sinh\left(\frac{L}{l_{\text{Cu}}}\right) + 2\left(\frac{R_{\text{NiFe}}}{R_{\text{Cu}}}\right) \left\{ \left(1 + \left(\frac{R_{\text{NiFe}}}{R_{\text{Cu}}} \right) \right) \left(1 + 2\left(\frac{R_{\text{M}}}{R_{\text{Cu}}}\right) \right) \exp\left(\frac{L}{l_{\text{Cu}}}\right) - 1 \right\}}, \quad (9)$$

where R_{M} is *spin resistance of the middle wire* which can be obtained from the ratio between the non-local spin valve signals with/without the middle wire [20] (see supplemental material for the detail). R_{NiFe} and R_{Cu} are the spin resistances of NiFe wire and Cu bridge wire, respectively. P is the spin polarization of NiFe, l_{Cu} is the spin diffusion length of the Cu bridge wire, L ($= 500$ nm) is the distance between middle wire and NiFe wire. $\overline{I_{\text{S,IEE}}}$ can thus be obtained as,

$$\overline{I_{\text{S,IEE}}} = \exp\left(-\frac{t_{\text{Cu}}}{l_{\text{M,Cu}}}\right) I_{\text{S,IEE}}, \quad (10)$$

where $l_{\text{M,Cu}}$ is the spin diffusion length of the Cu layer in the middle wire. The exponential factor represents the decay of the spin current in Cu layer in the middle wire, which becomes ~ 1 due to the

long $l_{\text{M,Cu}}$.

To calculate q , we need to know $j_{\text{c,DEE}}^{2\text{D}}$ in Eq. (4). This is in stark contrast to the calculation of λ , where we don't have to know $j_{\text{c,IEE}}^{2\text{D}}$ but assume that all the spin current is generated at the interface. We can estimate $j_{\text{c,DEE}}^{2\text{D}}$ by considering the parallel circuit of the 2D sheet resistance of the interface $R_{2\text{D}}$ and the sheet resistance of the middle wire $\rho_{\text{M}}/t_{\text{Cu}}$:

$$j_{\text{c,DEE}}^{2\text{D}} = \frac{x(\rho_{\text{M}}/t_{\text{Cu}})}{R_{2\text{D}} + \rho_{\text{M}}/t_{\text{Cu}}} I_{\text{c,DEE}}. \quad (11\text{a})$$

$$R_{2\text{D}} = \frac{m}{nt_{2\text{D}}e^2\tau_{\text{total}}}. \quad (11\text{b})$$

where n is the carrier density in Cu. By solving the 1D spin diffusion equations, we find $j_{\text{s,DEE}}^{3\text{D}}$ in Eq. (5) as follows (see supplemental materials for the deduction);

$$j_{\text{s,DEE}}^{3\text{D}} = \frac{\Delta R_{\text{DEE}} I_{\text{c,DEE}}}{2P\rho_{\text{M}}l_{\text{M,Cu}}} \left(a_1 \exp\left(-\frac{t_{\text{Cu}}}{l_{\text{M,Cu}}}\right) - a_2 \exp\left(\frac{t_{\text{Cu}}}{l_{\text{M,Cu}}}\right) \right), \quad (12\text{a})$$

$$a_1 = \left(\frac{1}{2} - \frac{R_{\text{M,Cu}}}{R_{\text{Cu}}}\right) \left(\frac{R_{\text{Cu}}}{R_{\text{NiFe}}} + 2\right) \exp\left(\frac{L}{l_{\text{Cu}}}\right) - \left(\frac{1}{2} + \frac{R_{\text{M,Cu}}}{R_{\text{Cu}}}\right) \left(\frac{R_{\text{Cu}}}{R_{\text{NiFe}}}\right) \exp\left(-\frac{L}{l_{\text{Cu}}}\right), \quad (12\text{b})$$

$$a_2 = \left(\frac{1}{2} + \frac{R_{\text{M,Cu}}}{R_{\text{Cu}}}\right) \left(\frac{R_{\text{Cu}}}{R_{\text{NiFe}}} + 2\right) \exp\left(\frac{L}{l_{\text{Cu}}}\right) - \left(\frac{1}{2} - \frac{R_{\text{M,Cu}}}{R_{\text{Cu}}}\right) \left(\frac{R_{\text{Cu}}}{R_{\text{NiFe}}}\right) \exp\left(-\frac{L}{l_{\text{Cu}}}\right). \quad (12\text{c})$$

Here, $R_{\text{M,Cu}}$ is the spin resistance of Cu in the middle wire. Note that $j_{\text{s,DEE}}^{3\text{D}}$ is different quantity from the spin current $j_{\text{s,DSHE}}^{3\text{D}}$ described as Eq. (S1) which we used to acquire θ_{DSHE}^* . For the following calculations, we assume a strong hybridization between the bulk and the interface [4,10], in which case τ_{total} may be the momentum scattering time of bulk $\tau_{\text{bulk}} = 10.6$ fs (see supplemental material for the estimation of τ_{bulk}) since the interface thickness $t_{2\text{D}}$ is equivalent to the width of the wave functions in the interface state. We adopted the typical interface thickness 0.4 nm for $t_{2\text{D}}$ [4,11].

We obtained negative values for λ and q at our $\text{Bi}_2\text{O}_3/\text{Cu}$ interfaces using Eqs. (8)-(12). The absolute values of λ and q as a function of t_{Cu} are shown in Fig. 3(b). We calculated τ_{IEE} , τ_{DEE} and α_{R} by using $m = 3.73 \times 10^{-31}$ kg and $v_{\text{F}} = 5.9 \times 10^5$ m/s which are the values of the surface state of Cu(111) [23]. We obtained $\tau_{\text{IEE}} \sim 13$ fs and $\tau_{\text{DEE}} \sim 53$ fs. The gradual increase of $|\alpha_{\text{R}}|$ with the Cu thickness levels off at a maximum value of ~ 0.46 eV $\cdot\text{\AA}$ when t_{Cu} is about 19 nm. This tendency is consistent with that at $\text{Bi}_2\text{O}_3/\text{Cu}$ interface reported in Refs. [8,11,12]. The Cu thickness dependence of α_{R} has been discussed in Ref. [11]. A smaller τ_{DEE} of ~ 16.6 fs was reported in $\text{Co}_{25}\text{Fe}_{75}$ (5 nm)/Cu (0-30 nm)/ Bi_2O_3 (20 nm) multilayers [11], which might be attributed to additional spin sinking from neighboring $\text{Co}_{25}\text{Fe}_{75}$ which is not the case for non-local lateral spin valve measurements. The spin ejection rate [11] $\eta = (1/\tau_{\text{DEE}})/(1/\tau_{\text{total}})$ is ~ 0.20 in our system, meaning that 20% of accumulated spins are ejected from the interface to the bulk.

As mentioned above, τ_{DEE} is about three times larger than τ_{IEE} in our system. This difference can be seen as a drop in the electrochemical potential $\Delta\mu(= \mu_1 - \mu_2)$ at the interface. The electrochemical potential as the function of the coordinate along the pass of spin current in the DEE measurement is illustrated in Fig. 4. The electrochemical potential μ_1 corresponds to the spin accumulation at the interface induced by applying $j_{\text{c,DEE}}^{2\text{D}}$ is given by

$$\mu_1 = \langle \delta S \rangle / \text{DOS}_{2\text{D}} \sim \frac{\pi \hbar \alpha_{\text{R}}}{emv_{\text{F}}^2} j_{\text{c,DEE}}^{2\text{D}}, \quad (14)$$

with the density of state at the interface $\text{DOS}_{2\text{D}} = m/\pi \hbar^2$. Equation (14) yields $\mu_1 \sim 40 \mu\text{eV}$. On the other hand, the electrochemical potential μ_2 in the Cu side of the middle wire can be estimated from V_{DEE} detected between NiFe and Cu bridge wires as follows,

$$\mu_2 = a_1 e^{-t_{\text{Cu}}/l_{\text{M,Cu}}} + a_2 e^{t_{\text{Cu}}/l_{\text{M,Cu}}}, \quad (15)$$

which yields $\mu_2 \sim 4 \mu\text{eV}$. In our system, only 10% of spin accumulation induced by $j_{\text{c,DEE}}^{2\text{D}}$ is ejected into the bulk, which is in the same order of the ejection ratio η of ~ 0.20 . Because of larger τ_{DEE} than τ_{IEE} , the spin ejection from the interface to the bulk is limited.

For example, at metal (111) surface of single crystal, the surface and bulk states at Fermi level are well defined [24,25]. In this case, τ_{total} , τ_{IEE} and τ_{DEE} are in the order of ps at low temperature because the residual resistivity of usual metallic single crystal is in order of $\text{n}\Omega\text{-cm}$ [26]. If this surface is used for the spin-to-charge current conversions, the ps-order τ_{IEE} will cause to increase λ but the ps-order τ_{DEE} decrease q . The similar situation is expected at the epitaxially grown interfaces [27]. An interface with large q doesn't necessarily exhibits large λ . Thus, we should consider both of λ and q to discuss the efficiency of the EE. This has been ignored in the discussion of Edelstein effects.

In summary, our experimental analyses by means of spin absorption methods revealed that the conversion coefficient of IEE is characterized by the momentum scattering time in the interface τ_{IEE} , while that of DEE is characterized by the spin ejection time τ_{DEE} . Both conversion coefficients λ and q are proportional to α_{R} . The sum of inverse relaxation times, $1/\tau_{\text{IEE}} + 1/\tau_{\text{DEE}}$ determines the total momentum relaxation time. Large τ_{IEE} and small τ_{DEE} are crucial for the high efficiency of EE. We also found that the *effective* spin Hall angle of $\text{Bi}_2\text{O}_3/\text{Cu}$ interface large and comparable to commonly used spin Hall material such as platinum.

References

- [1] V. M. Edelstein, Solid State Commun. **73**, 233 (1990).
- [2] J. Sinova, S. O. Valenzuela, J. Wunderlich, C. H. Back, and T. Jungwirth, Rev. Mod. Phys. **87**, 1213 (2015).
- [3] S. LaShell, B. A. McDougall, and E. Jensen, Phys. Rev. Lett. **77**, 3419 (1996).
- [4] J. C. R. Sánchez, L. Vila, G. Desfonds, S. Gambarelli, J. P. Attané, J. M. De Teresa, C. Magén,

- and A. Fert, *Nat. Commun.* **4**, 2944 (2013).
- [5] K. Shen, G. Vignale, and R. Raimondi, *Phys. Rev. Lett.* **112**, 096601 (2014).
- [6] K. Kondou, R. Yoshimi, A. Tsukazaki, Y. Fukuma, J. Matsuno, K. S. Takahashi, M. Kawasaki, Y. Tokura, and Y. Otani, *Nat. Phys.* **12**, 1027 (2016).
- [7] L. Liu, C.-F. Pai, Y. Li, H. W. Tseng, D. C. Ralph, and R. A. Buhrman, *Science* **336**, 555 (2012).
- [8] S. Karube, K. Kondou, and Y. C. Otani, *Appl. Phys. Express* **9**, 033001 (2016).
- [9] S. Karube, H. Idzuchi, K. Kondou, Y. Fukuma, and Y. Otani, *Appl. Phys. Lett.* **107**, 122406 (2015).
- [10] A. Yagmur, S. Karube, K. Uchida, K. Kondou, R. Iguchi, T. Kikkawa, Y. Otani, and E. Saitoh, *Appl. Phys. Lett.* **108**, 242409 (2016).
- [11] J. Kim, Y. T. Chen, S. Karube, S. Takahashi, K. Kondou, G. Tatara, and Y.C. Otani, *Phys. Rev. B* **96**, 140409(R) (2017).
- [12] H. Tsai, S. Karube, K. Kondou, N. Yamaguchi, F. Ishii, and Y. Otani, *Sci. Rep.* **8**, 5564 (2018).
- [13] P. Gambardella and I. M. Miron, *Philos. Trans. R. Soc. A Math. Phys. Eng. Sci.* **369**, 3175 (2011).
- [14] L. Moreschini, A. Bendounan, H. Bentmann, M. Assig, K. Kern, F. Reinert, J. Henk, C. R. Ast, and M. Grioni, *Phys. Rev. B - Condens. Matter Mater. Phys.* **80**, 035438 (2009).
- [15] E. Cappelluti, C. Grimaldi, and F. Marsiglio, *Phys. Rev. Lett.* **98**, 167002 (2007).
- [16] R. H. Silsbee, *J. Phys. Condens. Matter* **16**, R179 (2004).
- [17] S. Zhang and A. Fert, *Phys. Rev. B* **94**, 184423 (2016).
- [18] A. Slachter, F. L. Bakker, J. P. Adam, and B. J. Van Wees, *Nat. Phys.* **6**, 879 (2010).
- [19] L. Vila, T. Kimura, and Y.C. Otani, *Phys. Rev. Lett.* **99**, 226604 (2007).
- [20] Y. Niimi, H. Suzuki, Y. Kawanishi, Y. Omori, T. Valet, A. Fert, and Y. Otani, *Phys. Rev. B - Condens. Matter Mater. Phys.* **89**, 054401 (2014).
- [21] The developer of SpinFlow3D had gone bankrupt.
- [22] M. Isasa, M. C. Martínez-Velarte, E. Villamor, C. Magén, L. Morellón, J. M. De Teresa, M. R. Ibarra, G. Vignale, E. V. Chulkov, E. E. Krasovskii, L. E. Hueso, and F. Casanova, *Phys. Rev. B* **93**, 014420 (2016).
- [23] M. Hengsberger, F. Baumberger, H. J. Neff, T. Greber, and J. Osterwalder, *Phys. Rev. B - Condens. Matter Mater. Phys.* **77**, 085425 (2008).
- [24] J. Kliewer, R. Berndt, E. V Chulkov, V. M. Silkin, P. M. Echenique, and S. Crampin, *Science* (80-.). **288**, 1399 (2000).
- [25] A. A. Ünal, C. Tusche, S. Ouazi, S. Wedekind, C. T. Chiang, A. Winkelmann, D. Sander, J. Henk, and J. Kirschner, *Phys. Rev. B* **84**, 073107 (2011).
- [26] F. Sachslehner, *Phys. Status Solidi Basic Res.* **194**, 633 (1996).
- [27] E. Lesne, Y. Fu, S. Oyarzun, J. C. Rojas-Sánchez, D. C. Vaz, H. Naganuma, G. Sicoli, J. P.

Attané, M. Jamet, E. Jacquet, J. M. George, A. Barthélémy, H. Jaffrès, A. Fert, M. Bibes, and L. Vila, *Nat. Mater.* **15**, 1261 (2016).

Acknowledgement

We thank S. Karube and Y. Niimi for their constructive suggestions. This work was supported by a Grant-in-Aid for Scientific Research on Innovative Area, “Nano Spin Conversion Science” (Grant No. 26103002).

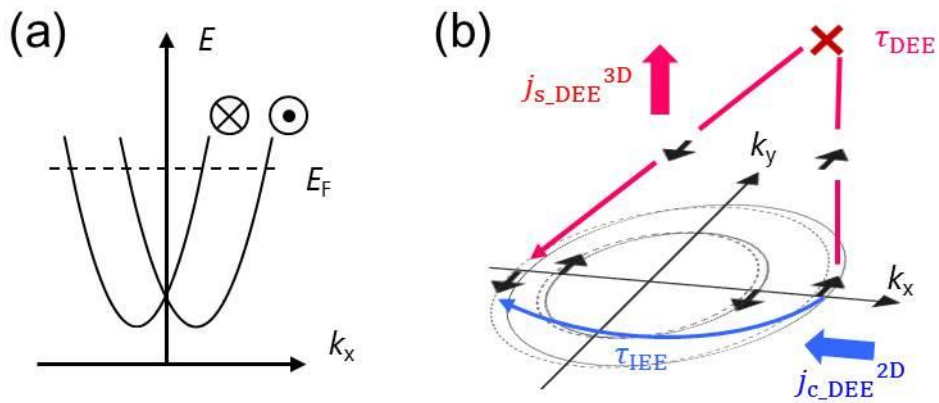


Figure 1: The concept of Edelstein effect. (a) Rashba splitting of parabolic band dispersion of interface state. (b) Fermi contour of (a) and illustration of direct Edelstein effect. A charge current along x direction create y -polarized spin accumulation. Blue arrow indicates a momentum scattering in the interface. Magenta arrow indicate the spin ejection across the interface. Red cross represents spin-flip in the bulk.

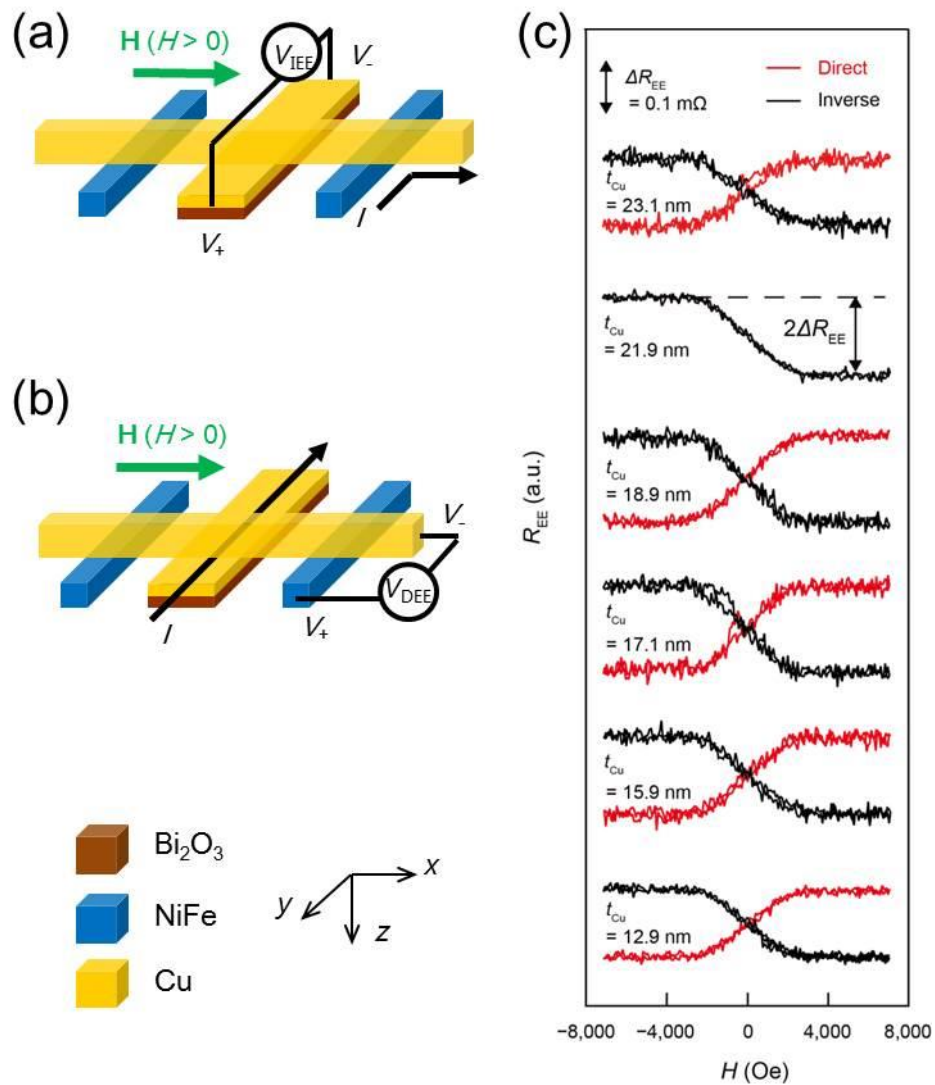


Figure 2: The measurement configuration for (a) inverse and (b) direct Edelstein effects with spin absorption method. (c) The Inverse (red lines) and direct (black lines) Edelstein resistances as a function of magnetic field at $\text{Bi}_2\text{O}_3/\text{Cu}$ interface with four different Cu thickness of $\text{Bi}_2\text{O}_3/\text{Cu}$ wire (The DEE for $t_{\text{Cu}} = 21.9 \text{ nm}$ was not measured).

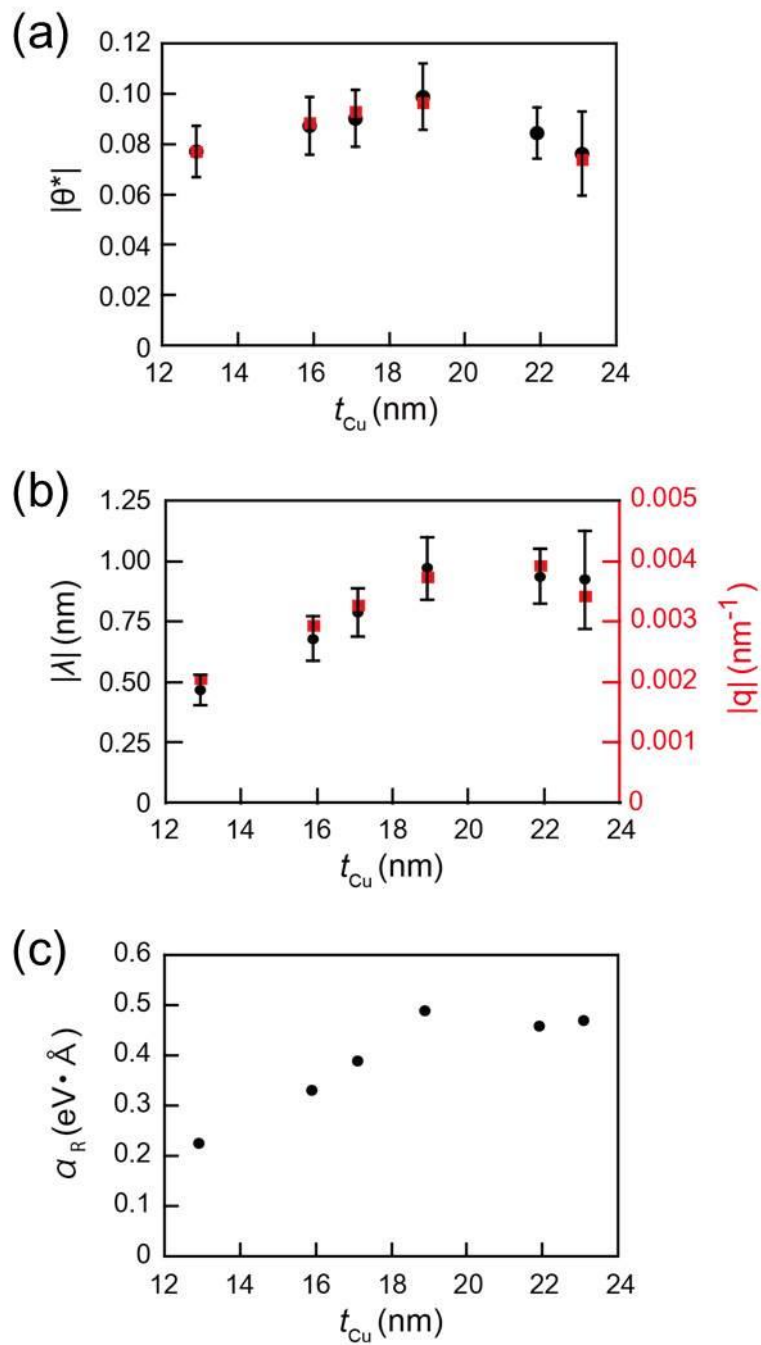


Figure 3: The *effective* spin Hall angle (a), conversion coefficients (b) and the Rashba parameter (c) of $\text{Bi}_2\text{O}_3/\text{Cu}$ as a function of Cu thickness of $\text{Bi}_2\text{O}_3/\text{Cu}$ wire. Black (red) points in (a) and (b) indicate the efficiency/coefficient for direct (inverse) effect. Error bars indicate the error propagation in the calculation.

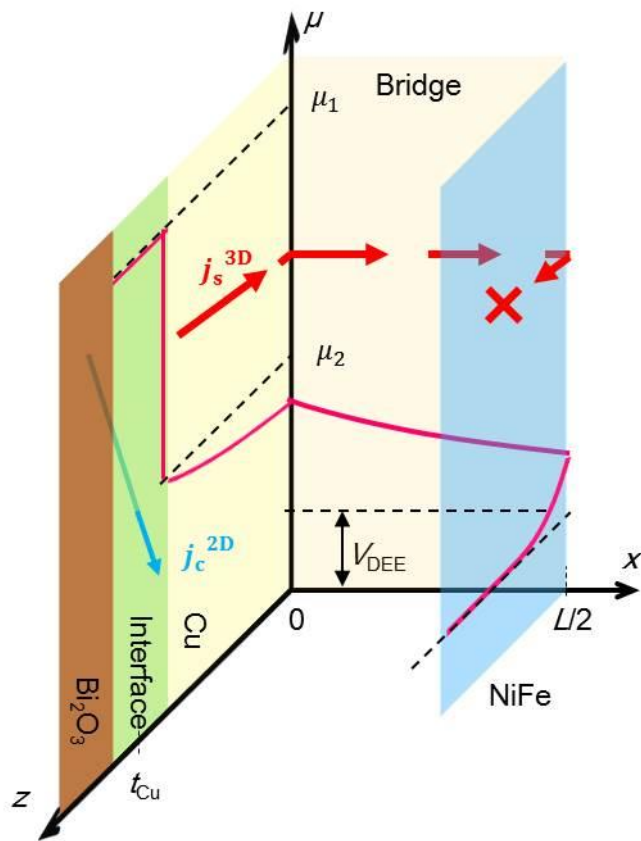
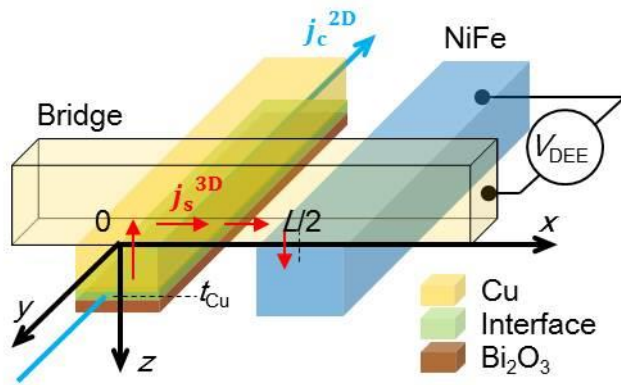


Figure 4: The measurement geometry of the DEE measurement (upper illustration) and the spatial distribution of electrochemical potential in non-equilibrium steady state in DEE measurement (lower illustration). Spin current $j_{s_DEE}^{3D}$ (red arrows) is given by the gradient of μ .

Supplemental material

Our device is a lateral spin valve where a Bi₂O₃/Cu middle wire is inserted in between two NiFe wires and bridged by a Cu wire (see Fig. 2 (a) and (b)). The nano wires were patterned by electron beam lithography on a thermally oxidized silicon substrate coated with a polymethyl-methacrylate resist. The NiFe wires are 100 nm wide, 30 nm thick and separated by 1 μm each other. The middle wire is 200 nm wide. Bi₂O₃ and Cu in the middle wire and NiFe were deposited by electron beam lithography under the pressure of a base pressure of 10⁻⁹ Torr. For the middle wire, Cu was deposited on 10-nm-thick Bi₂O₃. We prepared six samples with different Cu thickness in the middle wire (12.9 nm, 15.9 nm, 17.1 nm, 18.9 nm, 21.9 nm and 23.1 nm). The Cu bridge wire is 100 nm wide and 100 nm thick which was deposited by a heated tantalum boat under 10⁻¹⁰ Torr after the Ar ion beam etching for 30 seconds in order to clean the surfaces of NiFe wires and Cu of the middle wire. The prepared devices were coated by Al₂O₃ by AC sputtering to avoid the chemical reaction of the nano wires in air.

We discussed *effective* direct spin Hall angle where we assumed direct spin Hall effect in the middle wire instead of the direct Edelstein effect at the Bi₂O₃/Cu interface. The *effective* direct spin Hall angle θ_{DSHE}^* is defined as,

$$j_{s_{\text{DSHE}}}^{3\text{D}} \equiv \theta_{\text{DSHE}}^* j_{c_{\text{DSHE}}}^{3\text{D}}, \quad (\text{S1})$$

where, $j_{s_{\text{DSHE}}}^{3\text{D}}$ is the spin current generated by the *effective* spin Hall effect and $j_{c_{\text{DSHE}}}^{3\text{D}}$ is the charge current which flows the middle wire. Note that $j_{s_{\text{DSHE}}}^{3\text{D}}$ is different quantity from $j_{s_{\text{DEE}}}^{3\text{D}}$; according to the definition, $j_{s_{\text{DSHE}}}^{3\text{D}}$ should be generated at each point in the middle wire, while $j_{s_{\text{DEE}}}^{3\text{D}}$ arises from the spin accumulation in the interface. We evaluated $j_{s_{\text{DSHE}}}^{3\text{D}}$ and θ_{DSHE}^* as follows using 1D diffusion model (see Fig. S1). In direct spin Hall effect, the total spin current $j_{\text{total}}^{3\text{D}}$ is represented by the summation of $j_{s_{\text{DSHE}}}^{3\text{D}}$ and the gradient of the electrochemical potential as follows.

$$j_{\text{total}}^{3\text{D}} = j_{s_{\text{DSHE}}}^{3\text{D}} - \frac{1}{2e\rho_{\text{Cu}}} \frac{\partial}{\partial z} \mu. \quad (\text{S2})$$

We used the boundary condition, $j_{\text{total}}^{3\text{D}} = 0$ at $z = t_{\text{Cu}}$ and solved the diffusion equations. As the result θ_{DSHE}^* was deduced as,

$$\theta_{\text{DSHE}}^* = \frac{j_{s_{\text{DSHE}}}^{3\text{D}}}{j_{c_{\text{DSHE}}}^{3\text{D}}} = \frac{Vt_{\text{Cu}}}{xIPR_{\text{M}}W_{\text{Cu}} \tanh(t_{\text{Cu}}/\lambda_{\text{M}})} \frac{1}{(2 - e^{-t_{\text{M}}/\lambda_{\text{M}}} - e^{t_{\text{M}}/\lambda_{\text{M}}})} \\ \times \left\{ -(b_1 - b_2) \exp\left(\frac{-t_{\text{Cu}}}{\lambda_{\text{M}}}\right) + (b_3 - b_4) \exp\left(\frac{t_{\text{Cu}}}{\lambda_{\text{M}}}\right) \right\}, \quad (\text{S3a})$$

$$b_1 = \left(\frac{1}{2} - \tanh(t_{\text{Cu}}/\lambda_{\text{M}}) \frac{R_{\text{M}}}{R_{\text{Cu}}}\right) \left(\frac{R_{\text{Cu}}}{R_{\text{NiFe}}} + 2\right) \exp\left(\frac{L}{\lambda_{\text{Cu}}}\right), \quad (\text{S3b})$$

$$b_2 = \left(\frac{1}{2} + \tanh(t_{\text{Cu}}/\lambda_{\text{M}}) \frac{R_{\text{M}}}{R_{\text{Cu}}}\right) \left(\frac{R_{\text{Cu}}}{R_{\text{NiFe}}}\right) \exp\left(-\frac{L}{\lambda_{\text{Cu}}}\right), \quad (\text{S3c})$$

$$b_3 = \left(\frac{1}{2} + \tanh(t_{\text{Cu}}/\lambda_{\text{M}}) \frac{R_{\text{M}}}{R_{\text{Cu}}}\right) \left(\frac{R_{\text{Cu}}}{R_{\text{NiFe}}} + 2\right) \exp\left(\frac{L}{\lambda_{\text{Cu}}}\right), \quad (\text{S3d})$$

$$b_4 = \left(\frac{1}{2} - \tanh(t_{\text{Cu}}/\lambda_{\text{M}}) \frac{R_{\text{M}}}{R_{\text{Cu}}}\right) \left(\frac{R_{\text{Cu}}}{R_{\text{NiFe}}}\right) \exp\left(-\frac{L}{\lambda_{\text{Cu}}}\right). \quad (\text{S3e})$$

The values of θ_{DSHE}^* plotted in Fig. 3 (a) were obtained by these equation.

We had fabricated the spin valve without the $\text{Bi}_2\text{O}_3/\text{Cu}$ line. *Spin resistance of the middle wire* R_{M} can be obtained from the ratio between the non-local spin valve signals with and without the middle wire as described in Ref. [1]. The measurement configurations are shown in Fig. 2S (a). Figure S2 (b) shows the typical results of our non-local spin valve measurements where $t_{\text{Cu}} = 17.1$ nm. The measurements were performed in all of the samples and R_{M} were obtained for each sample.

The resistance of $\text{Cu}/\text{Bi}_2\text{O}_3$ wire has been measured by four-terminal method at 10 K. The resistivity of Cu as a function of t_{Cu} is shown in Fig. S3. When the dimension of Cu nanowire is smaller than the electron mean free pass l_{mfp} , the measured resistivity is different from the intrinsic (bulk) resistivity due to the scattering at the surfaces and grain boundaries. We have estimated the resistivity of bulk Cu ρ_0 by the fitting of the experimental data with the following equation [2-3],

$$\rho = \rho_0 \left\{ \frac{1}{3} / \left[\frac{1}{3} - \frac{a}{2} + a^2 - a^3 \ln \left(1 + \frac{1}{a} \right) \right] + \frac{3}{8} C (1-p) \frac{1+\text{AR}}{\text{AR}} \frac{l_{\text{mfp}}}{t_{\text{Cu}}-h} \right\}, \quad (\text{S4a})$$

$$a = \frac{l_{\text{mfp}} R}{d (1-R)}, \quad (\text{S4b})$$

where, C is a constant with value 1.2 for a rectangular cross section, p is specularity parameter, AR is the aspect ratio and h is the roughness of the surface, R is reflectivity coefficient at grain boundaries and d is the average distance between grain boundaries. The parameters for the fitting in Fig. S3 are as follows: $p = 0$, $h = 7$ nm, $R = 0.25$ and $\rho_0 l_{\text{mfp}} = 6.6 \times 10^{-16} \Omega\text{m}^2$. We have assumed that the average grain size is equal to t_{Cu} ($d = t_{\text{Cu}}$) [2]. We obtained $\rho_0 = 4.0 \mu\Omega \cdot \text{cm}$ from the fitting. By using Drude model, we obtained the momentum scattering time in the bulk $\tau_{\text{bulk}} = 10.6$ fs.

By using 1D spin diffusion model, we deduce Eq. (12): the spin current arises from the $\text{Bi}_2\text{O}_3/\text{Cu}$ interface as the function of the Edelstein voltage V_{DEE} . The model we consider is illustrated in Fig. S4. In general, the spin diffusion equation is written as

$$\nabla^2(\mu_{\uparrow} - \mu_{\downarrow}) = \frac{1}{l^2}(\mu_{\uparrow} - \mu_{\downarrow}), \quad (\text{S5a})$$

$$\nabla^2(\sigma^{\uparrow}\mu_{\uparrow} - \sigma^{\downarrow}\mu_{\downarrow}) = 0, \quad (\text{S5b})$$

$$j_{\uparrow,\downarrow} = -\frac{\sigma_{\uparrow,\downarrow}}{e} \nabla \mu_{\uparrow,\downarrow}, \quad (\text{S5c})$$

$$I_{\text{S}} = j_{\uparrow} - j_{\downarrow}, \quad (\text{S5d})$$

where μ_{σ} is electrochemical potential for spin up ($\sigma = \uparrow$) and spin down ($\sigma = \downarrow$), σ^{σ} is spin dependent electrical conductivity and j_{σ} is the current density for spin channel for spin channel σ ($\sigma = \uparrow, \downarrow$).

In region (I) (see Fig. S4), the general solution of Eq. (S5a) is

$$\begin{aligned}\mu_{\uparrow}^{\text{I}} - \mu_{\downarrow}^{\text{I}} &= a_1 e^{-z/l_{\text{M,Cu}}} + a_2 e^{z/l_{\text{M,Cu}}}, \\ \mu_{\uparrow}^{\text{I}} + \mu_{\downarrow}^{\text{I}} &= 0.\end{aligned}$$

Thus,

$$\begin{aligned}\mu_{\uparrow}^{\text{I}} &= \frac{1}{2}(a_1 e^{-z/l_{\text{M,Cu}}} + a_2 e^{z/l_{\text{M,Cu}}}), \\ \mu_{\downarrow}^{\text{I}} &= -\frac{1}{2}(a_1 e^{-z/l_{\text{M,Cu}}} + a_2 e^{z/l_{\text{M,Cu}}}), \\ j_{\uparrow}^{\text{I}} &= \frac{\sigma_{\text{M}}}{4el_{\text{M,Cu}}}(a_1 e^{-z/l_{\text{M,Cu}}} - a_2 e^{z/l_{\text{M,Cu}}}), \\ j_{\downarrow}^{\text{I}} &= -\frac{\sigma_{\text{M}}}{4el_{\text{M,Cu}}}(a_1 e^{-z/l_{\text{M,Cu}}} - a_2 e^{z/l_{\text{M,Cu}}}),\end{aligned}$$

$$I_{\text{S}}^{\text{I}} = -\frac{1}{2eR_{\text{M,Cu}}}(a_1 e^{-z/l_{\text{M,Cu}}} - a_2 e^{z/l_{\text{M,Cu}}}), \quad (\text{S6C})$$

$$R_{\text{M,Cu}} = \frac{\rho_{\text{M}} l_{\text{M,Cu}}}{w_{\text{M}} w_{\text{bridge}}},$$

where w_{bridge} is the width of bridge wire and σ_{M} is the electric conductivity of the middle wire.

In region (II),

$$\begin{aligned}\mu_{\uparrow}^{\text{II}} - \mu_{\downarrow}^{\text{II}} &= b_1 e^{-x/l_{\text{Cu}}} + b_2 e^{(x-L)/l_{\text{Cu}}}, \\ \mu_{\uparrow}^{\text{II}} + \mu_{\downarrow}^{\text{II}} &= 0,\end{aligned}$$

Thus,

$$\begin{aligned}\mu_{\uparrow}^{\text{II}} &= \frac{1}{2}(b_1 e^{-x/l_{\text{Cu}}} + b_2 e^{(x-L)/l_{\text{Cu}}}), \\ \mu_{\downarrow}^{\text{II}} &= -\frac{1}{2}(b_1 e^{-x/l_{\text{Cu}}} + b_2 e^{(x-L)/l_{\text{Cu}}}), \\ j_{\uparrow}^{\text{II}} &= \frac{\sigma_{\text{Cu}}}{4e\lambda_{\text{Cu}}}(b_1 e^{-x/l_{\text{Cu}}} - b_2 e^{(x-L)/l_{\text{Cu}}}), \\ j_{\downarrow}^{\text{II}} &= -\frac{\sigma_{\text{Cu}}}{4e\lambda_{\text{Cu}}}(b_1 e^{-x/l_{\text{Cu}}} - b_2 e^{(x-L)/l_{\text{Cu}}}), \\ I_{\text{S}}^{\text{II}} &= -\frac{1}{2eR_{\text{Cu}}}(b_1 e^{-x/l_{\text{Cu}}} - b_2 e^{(x-L)/l_{\text{Cu}}}),\end{aligned}$$

$$R_{\text{Cu}} = \frac{\rho_{\text{Cu}} l_{\text{Cu}}}{w_{\text{bridge}} t_{\text{bridge}}},$$

where t_{bridge} is the thickness of the bridge wire, σ_{Cu} (ρ_{Cu}) is the electric conductivity (resistivity) of the bridge wire.

In region (III),

$$\begin{aligned}\mu_{\uparrow}^{\text{III}} - \mu_{\downarrow}^{\text{III}} &= c_1 e^{-z/l_{\text{NiFe}}}, \\ \sigma_{\text{NiFe}}^{\uparrow} \mu_{\uparrow}^{\text{III}} + \sigma_{\text{NiFe}}^{\downarrow} \mu_{\downarrow}^{\text{III}} &= eV_{\text{DEE}} \sigma_{\text{NiFe}}, \\ \sigma_{\text{NiFe}} &= \sigma_{\text{NiFe}}^{\uparrow} + \sigma_{\text{NiFe}}^{\downarrow}.\end{aligned}$$

Thus,

$$\mu_{\uparrow}^{\text{III}} = eV_{\text{DEE}} + c_1 \frac{\sigma_{\text{NiFe}}^{\downarrow}}{\sigma_{\text{NiFe}}} e^{-z/l_{\text{NiFe}}},$$

$$\mu_{\downarrow}^{\text{III}} = eV_{\text{DEE}} - c_1 \frac{\sigma_{\text{NiFe}}^{\uparrow}}{\sigma_{\text{NiFe}}} e^{-z/l_{\text{NiFe}}},$$

$$j_{\uparrow}^{\text{III}} = \frac{\sigma_{\text{NiFe}}^{\uparrow} \sigma_{\text{NiFe}}^{\downarrow} c_1}{e \lambda_{\text{NiFe}} \sigma_{\text{NiFe}}} e^{-z/l_{\text{NiFe}}},$$

$$j_{\downarrow}^{\text{III}} = -\frac{\sigma_{\text{NiFe}}^{\uparrow} \sigma_{\text{NiFe}}^{\downarrow} c_1}{e l_{\text{NiFe}} \sigma_{\text{NiFe}}} e^{-z/l_{\text{NiFe}}},$$

$$I_S^{\text{III}} = -\frac{1}{2eR_{\text{NiFe}}} e^{-z/l_{\text{NiFe}}},$$

$$R_{\text{NiFe}} = \frac{l_{\text{NiFe}} \sigma_{\text{NiFe}}}{4\sigma_{\text{NiFe}}^{\uparrow} \sigma_{\text{NiFe}}^{\downarrow} w_{\text{bridge}} w_{\text{NiFe}}},$$

$$(1 - P_{\text{NiFe}}^2) = \frac{4\sigma_{\text{NiFe}}^{\uparrow} \sigma_{\text{NiFe}}^{\downarrow}}{\sigma_{\text{NiFe}}^2},$$

where P_{NiFe} is the spin polarization of NiFe and σ_{NiFe} is the electric conductivity of NiFe.

In region (IV),

$$\mu_{\uparrow}^{\text{IV}} - \mu_{\downarrow}^{\text{IV}} = d_1 e^{-(x-L)/l_{\text{Cu}}},$$

$$\mu_{\uparrow}^{\text{IV}} + \mu_{\downarrow}^{\text{IV}} = 0,$$

Thus,

$$\mu_{\uparrow}^{\text{IV}} = \frac{1}{2} d_1 e^{-(x-L)/l_{\text{Cu}}},$$

$$\mu_{\downarrow}^{\text{IV}} = -\frac{1}{2} d_1 e^{-(x-L)/l_{\text{Cu}}},$$

$$j_{\uparrow}^{\text{IV}} = \frac{\sigma_{\text{Cu}} d_1}{4e l_{\text{Cu}}} e^{-(x-L)/l_{\text{Cu}}},$$

$$j_{\downarrow}^{\text{IV}} = -\frac{\sigma_{\text{Cu}} d_1}{4e l_{\text{Cu}}} e^{-(x-L)/l_{\text{Cu}}},$$

$$I_S^{\text{IV}} = \frac{d_1}{2eR_{\text{Cu}}} e^{-(x-L)/l_{\text{Cu}}},$$

We used boundary conditions as follows.

At $x=0, z=0$,

$$I_S^{\text{I}} = -2I_S^{\text{II}},$$

$$\mu_{\uparrow}^{\text{I}} = \mu_{\uparrow}^{\text{II}},$$

$$(\mu_{\downarrow}^{\text{I}} = \mu_{\downarrow}^{\text{II}}).$$

At $x=L, z=0$,

$$I_S^{\text{II}} = I_S^{\text{III}} + I_S^{\text{IV}},$$

$$\mu_{\uparrow}^{\text{II}} = \mu_{\uparrow}^{\text{III}} = \mu_{\uparrow}^{\text{IV}},$$

$$\mu_{\downarrow}^{\text{II}} = \mu_{\downarrow}^{\text{III}} = \mu_{\downarrow}^{\text{IV}}.$$

We obtain Eq. (12) when we eliminated unknown quantities b_1 , b_2 , c_1 , d_1 by solving the simultaneous equations.

References

- [1] Y. Niimi, H. Suzuki, Y. Kawanishi, Y. Omori, T. Valet, A. Fert, and Y. Otani, Phys. Rev. B - Condens. Matter Mater. Phys. **89**, 054401 (2014)
- [2] W. Steinhögl, G. Schindler, G. Steinlesberger, M. Traving, and M. Engelhardt, J. Appl. Phys. **97**, 023706 (2005)
- [3] W. Steinhögl, G. Schindler, G. Steinlesberger, and M. Engelhardt, Phys. Rev. B. **66**, 075414 (2002)

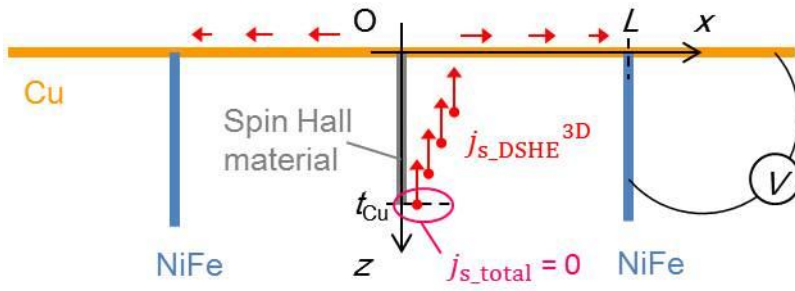


Figure S1: The illustration of 1D diffusion model of direct spin Hall effect detected by non-local spin valve structure.

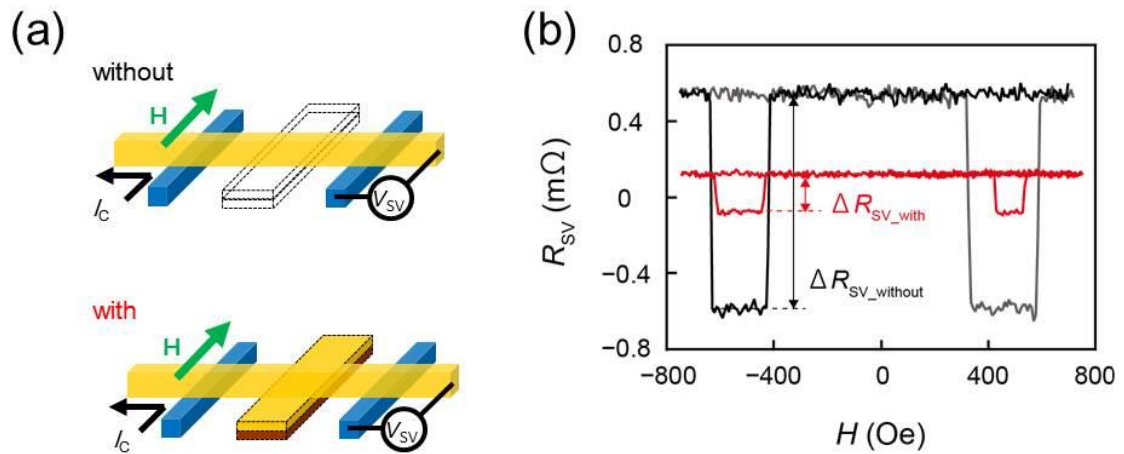


Figure S2: Non-local spin valve measurement with and without $\text{Bi}_2\text{O}_3/\text{Cu}$ wire. (a) The measurement configurations. (b) The typical results with (red line) and without (black line) $\text{Bi}_2\text{O}_3/\text{Cu}$ wire.

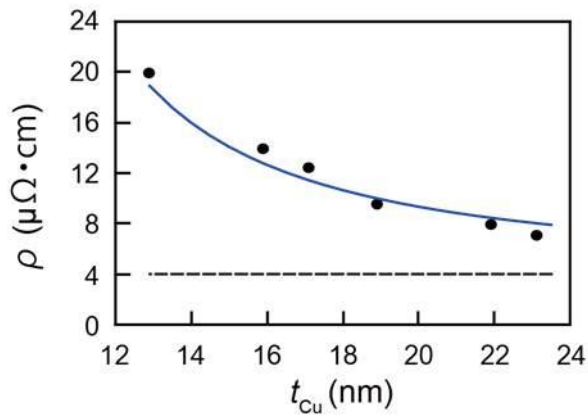


Figure S3: The resistivity of Cu wire as a function of the Cu thickness. Dots are the experimental data points. Blue solid line is the fitting. Black dashed line is the bulk resistivity.

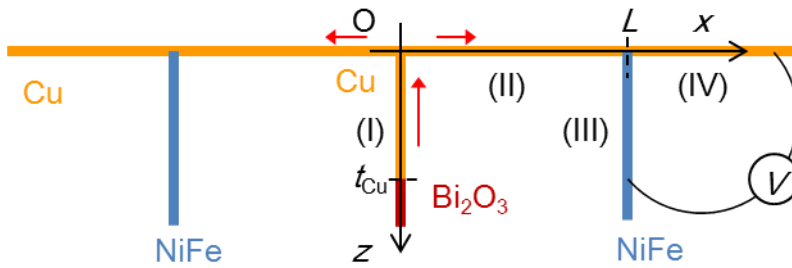


Figure S4: The illustration of 1D diffusion model of direct Edelstein effect detected by non-local spin valve structure.